

Strong continuum-continuum couplings in the direct ionization of Ar and He atoms by 6-MeV/u U^{38+} and Th^{38+} projectiles

D. Schneider* and D. DeWitt

Lawrence Livermore National Laboratory, Livermore, California 94550

A. S. Schlachter

Lawrence Berkeley Laboratory, Berkeley, California 94720

R. E. Olson

University of Missouri, Rolla, Missouri 65401

W. G. Graham

Queens University, Belfast, Northern Ireland

J. R. Mowat

North Carolina State University, Raleigh, North Carolina 27695

R. D. DuBois

Battelle Institute, Pacific Northwest Laboratory, Richland, Washington 99538

D. H. Loyd

Angelo State University, San Angelo, Texas 76909

V. Montemayor and G. Schiwietz

Hahn-Meitner-Institut, 1000 Berlin 39, West Germany

(Received 30 January 1989; revised manuscript received 24 April 1989)

Doubly differential cross sections have been measured as a function of the electron energy and observation angle for electron emission following collisions of 6-MeV/u U^{38+} and Th^{38+} on He and Ar. The electron-emission data show an enhancement at forward angles and a decrease at backward angles with respect to scaled-cross-section results based on the Born approximation. Comparison with classical-trajectory Monte Carlo calculations suggests that the deviation from the Born approximation can be explained by continuum-continuum couplings. By comparing with previously published data, we found that the forward enhancement as well as the backward decrease follow a q/v_p (q, v_p are the projectile charge and velocity) scaling.

I. INTRODUCTION

Continuum-electron emission in light-ion impact has been systematically investigated via measurements of absolute doubly differential cross sections in collisions of 50-keV to 5-MeV H^+ on He and Ar (Refs. 1-7). It was shown that, for fast collisions ($E_p > 1$ MeV/u), the plane-wave Born approximation (PWBA) predicts electron-production cross sections rather accurately. Only recently has it been demonstrated that investigations of doubly differential electron-emission cross sections and probabilities from fast-ion-atom collisions are a sensitive measure of the dynamics of the ionization process occurring in the collision.⁸⁻¹⁶ Measurements of differential ionization cross sections at high incident energies are able to test theoretical models in a large range of impact parameters even without any coincidence conditions. The adiabatic distance $r_{ad} = v_p / \Delta E$ (in a.u.) which is related to the minimum momentum transfer in the PWBA, might be

relatively small, since for high-electron energies the projectile speed v_p is smaller than the corresponding energy transfer ΔE in atomic units. Thus, at high-electron energies the ionization cross sections will be influenced by higher-order effects,^{9,14} especially when the projectile charge is high.^{10,13}

Recently, an enhanced-forward and reduced-backward electron emission compared to PWBA predictions (utilizing sophisticated wave functions) was found in collisions of energetic, highly charged projectiles with He and Ar atoms.¹⁰⁻¹² A mechanism which accounts for an enhancement of the doubly differential cross sections for electrons with nearly projectile velocity is the so-called electron capture to the projectile continuum (ECC). This mechanism might be described by the first Born approximation where the initial state is a target-centered bound state and the final state is a projectile-centered continuum state.¹⁷⁻¹⁹ For higher-electron velocities where the Coulomb forces of both nuclei are comparable this con-

cept breaks down,⁸⁻¹⁴ and one may speak of a two-center electron emission.^{10,11,19} The corresponding enhancement of the forward electron emission may then only be described by higher-order theories such as the continuum-distorted-wave-eikonal approximation^{11,13} (CDW-EIS) or classical-trajectory Monte Carlo (CTMC) models.^{10,14,20-22}

In order to avoid influences on the emission process due to molecular processes or binding effects, we performed the present study for high incident energies (6 MeV/u), where the projectile speed v_p was much higher than the mean orbital velocity v_i of the target electrons in the ground state. A high incident projectile charge was chosen ($Z_p=38$) in order to investigate the Z_p dependence of the forward enhancement of electron emission in comparison with previously published intermediate Z_p data. Comparison will also be made between experiments, PWBA predictions, and results from two different CTMC codes.

II. EXPERIMENTAL METHOD

Absolute doubly differential cross sections were determined for electron emission following collisions of 6-MeV/u U^{38+} on Ar and He at angles in the range 20–150°. Additional data for collisions of 6-MeV/u Th^{38+} on Ar are shown. The experiments were performed at the SuperHILAC accelerator at the Lawrence Berkeley Laboratory.

The experimental setup for continuum- (or secondary-) electron spectroscopy in energetic heavy-ion-atom collisions, shown in Fig. 1, has been recently installed. Its basic design is similar to the one described in Ref. 3. It consists of a magnetically shielded chamber reducing the Earth's magnetic field by more than a factor of 100. Ion beams of 6-MeV/u U^{38+} and Th^{38+} , produced by stripping a fast ion beam in a carbon foil, were charge-state selected, collimated, and focused at the center of the target chamber, where they crossed an atomic Ar or He tar-

get beam from a gas jet. The pressure in the target region was about 10^{-2} Torr over a length of about 3 mm. It was established that this target thickness ensures single-collision conditions. Electrons ejected from the target region were analyzed by an electrostatic 45° parallel-plate analyzer with a solid angle of 4×10^{-3} sr, an energy resolution of 9%, and an angular acceptance of $\pm 4^\circ$. The secondary-electron emission was observed between 20° and 150° in an energy range between 10 and 5000 eV. A peak at about 180 eV, which becomes increasingly distinct from the background as the observation angle increases, results from Ar L-shell Auger-electron emission following L-shell ionization accompanied by multiple M-shell ionization (see Fig. 5). The data at 150° for Ar show a distinct structure due to Ar L-shell Auger electron emission. The continuum under the Ar L-shell Auger peak was subtracted and the cross section was deduced from the integrated yield. The cross section for total L-shell ionization was calculated using the Born approximation with appropriate screening,^{23,24} which yielded a value of 1.71×10^{-15} cm². The experimentally deduced cross section for Ar L-Auger production agrees with theory within the accuracy given for the absolute values of $\pm 40\%$ if a fluorescence yield of about 30% is taken into account. This value is in agreement with the observed centroid energy for the intensity due to Ar L-shell Auger electron emission. The Ar L-Auger electron production cross section was then used to normalize the continuum cross section. The continuum electron spectra were corrected for background contributions determined from measurements without a gas target. The relative uncertainty of the doubly differential cross section is about 30%, and absolute values have an uncertainty of about 40%.

III. THEORETICAL MODELS

In this paper we present results from two different theories: PWBA (plane-wave Born approximation) and

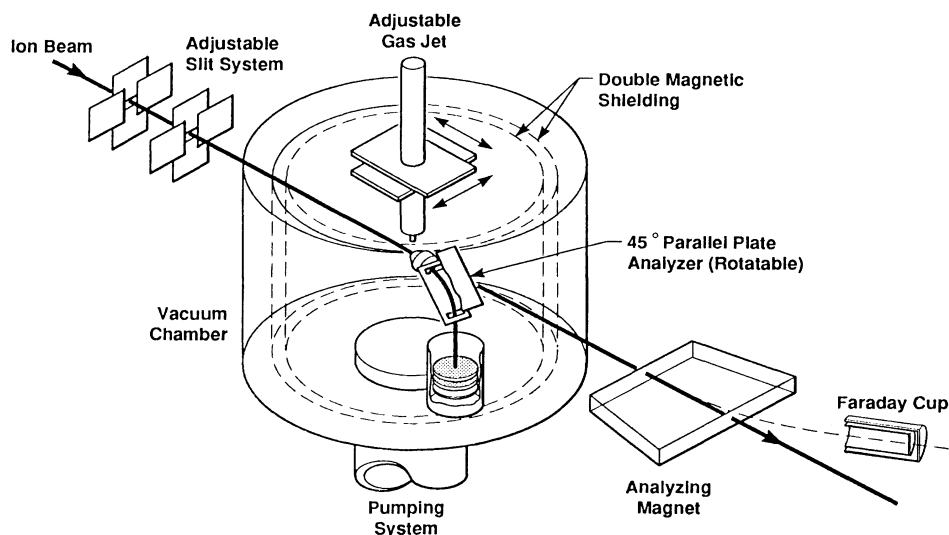


FIG. 1. Experimental setup for electron spectroscopy at the SuperHILAC accelerator at Lawrence Berkeley Laboratory.

CTMC (classical-trajectory Monte Carlo calculations). The PWBA results by Manson⁴ shown in this paper are taken from Ref. 10 and scaled from 5 MeV/u to 6 MeV/u. It is known^{7,23} that differential PWBA cross sections scale as $Z_p^2 \ln(v_p^2)/v_p^2$ for low-electron energies and as Z_p^2/v_p^2 for high-electron energies. Since the present investigation was performed for final-electron energies larger than the outer-shell binding energies of the target atoms, we used the latter scaling. The fully quantum-mechanical PWBA is a first-order theory, and treats the ionization mechanism as being a sudden process. Thus, although highly sophisticated Hartree-Fock wave functions were utilized and continuum partial waves up to $l = 16$ were taken into account, no allowance is made for polarization effects such as, e.g., continuum-continuum couplings.

We also present results from two different CTMC codes. Since the CTMC treats the particle motion classically, a comment on the validity of such calculations might be in order. In a CTMC calculation the coordinate and momentum distribution is represented by a statistical ensemble. The quantum-mechanical time-dependent wave function can be viewed as being projected onto a large set of independent wave packets. The mean position and mean velocity of these wave packets follow exactly Newton's second law, but a full solution of the time-dependent Schrödinger equation would include interference effects between overlapping wave packets. Neglecting these interferences, one may solve the classical Hamilton equations for independent probability particles (wave packets). This concept breaks down for low-incident energies ($v_p \ll v_i$) (Ref. 20) where the classical density distribution and binding energies disagree with the quantum-mechanical molecular-orbital wave functions and binding energies. This can be understood as a result of the neglect of interferences for probability particles in the initial state.

For high incident energies, classical theories become invalid if the momentum transfer is very low, and optically allowed dipole transitions dominate the spectrum of all emitted electrons. The condition for this to happen seems to be $r_{ad} > r_i$, where r_i is the classical turning point for bound electrons. Thus classical ionization probabilities should be accurate if $v_p I < \Delta E Z_T$, where I is the ionization potential in atomic units and Z_T is an

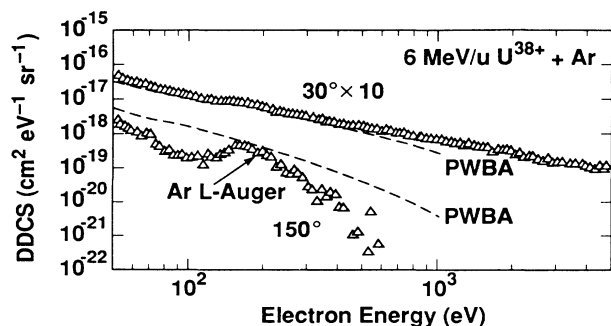


FIG. 2. Experimental doubly-differential ionization cross sections for 6-MeV/u $U^{38+} + Ar$ collisions compared to scaled PWBA cross sections taken from Ref. 4.

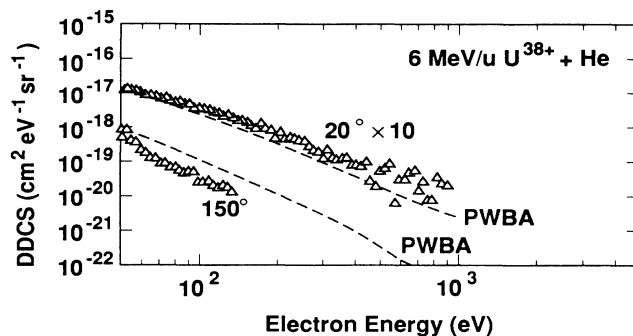


FIG. 3. Experimental doubly-differential ionization cross section for 6-MeV/u $U^{38+} + He$ collisions compared to scaled PWBA cross sections.

effective target nuclear charge. For 6-MeV/u $U^{38+} + Ar$ collisions there should be no significant differences between CTMC results and exact solutions of the time-dependent Schrödinger equation (going beyond first-order solutions of the PWBA). Thus the CTMC results should be superior to the PWBA cross sections whenever polarization effects are of importance.

The differences between the two CTMC codes used in this investigation are as follows. The n -body CTMC (n CTMC) (Ref. 14) treats all 18 Ar target electrons independently, neglecting electron-electron correlations determined by the Coulomb operator $1/(|r_j - r_k|)$ but solves the equations of motion for all electrons (r_j and r_K are electron coordinates) simultaneously as each electron moves in the Coulomb field of the target nucleus. Thus the projectile motion will be influenced by the interaction with n electrons. However, the exact treatment of the projectile motion is expected to be of minor importance for the present investigation.

The frozen-core self-consistent-field CTMC (SCTMC)²¹ solves the classical equation of motion for each electron (or each shell) separately, but the electronic motion was evaluated using a screened (classical self-consistent-field) non-Coulomb target potential. Thus the initial momentum distribution used in the SCTMC is very similar to the quantum-mechanical Hartree-Fock solution,²¹ and the initial momentum distribution in the n CTMC is ex-

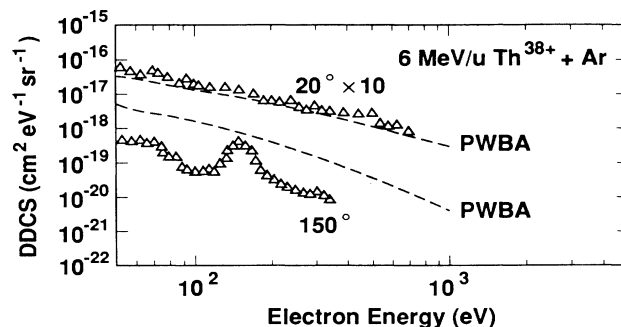


FIG. 4. Experimental doubly-differential ionization cross sections for 6-MeV/u $Th^{38+} + Ar$ collision compared to scaled PWBA cross sections taken from Ref. 4.

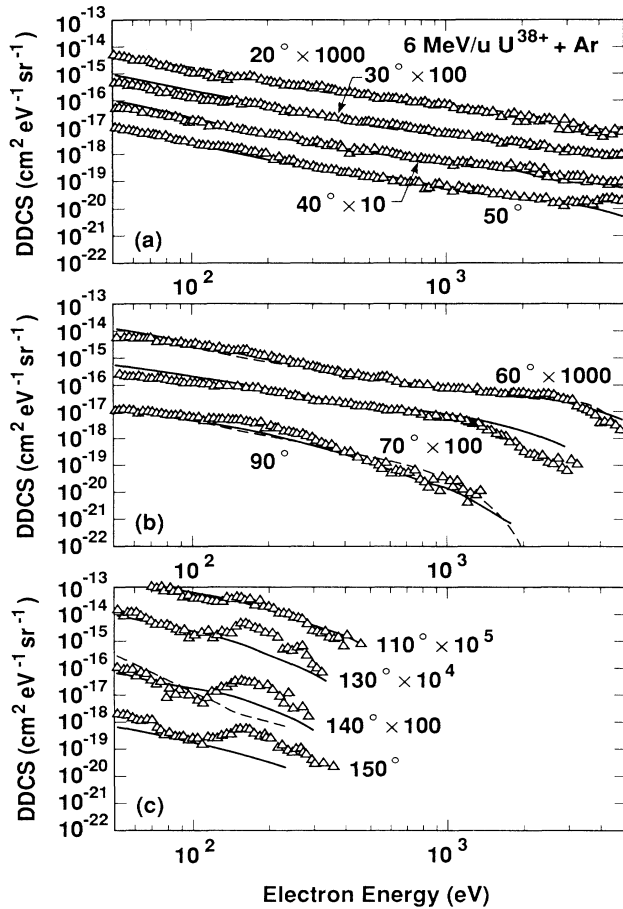


FIG. 5. Experimental doubly-differential ionization cross sections for 6-MeV/u $U^{38+} + Ar$ collisions compared to two different classical-trajectory Monte Carlo calculations: $nCTMC$ (dashed lines) and $SCTMC$ (solid lines). $nCTMC$ results are shown only for the electron-emission angles 20° , 30° , 60° , 90° , and 140° .

actly the same as the quantum-mechanical density distribution for a hydrogenlike target potential. Therefore, the $SCTMC$ should be superior to the $nCTMC$ whenever the initial momentum distribution is important to describe the ionization process.²¹ However, the $SCTMC$ will inadequately follow high stages of ionization at small impact parameters since the energy deposition is not correctly portrayed. For 0° electron ejection (cusp electrons) both approaches seem to be fairly accurate.^{15,16,21,25}

IV. RESULTS AND DISCUSSION

Experimental doubly differential cross sections (DDCS) for 6-MeV/u collisions of U^{38+} and Th^{38+} on Ar and He are compared to results from PWBA calculations⁴ in Figs. 2–4. It is obvious that the PWBA underestimates the ionization cross section for forward electron ejection and overestimates these at backward angle. This effect was also observed in earlier investigations of $H^+ + He$ collisions, and was attributed to the electron capture to the continuum. However, for the present case of fast highly charged uranium projectiles, the expected enhancement of the singly differential cross sections $d\sigma/dE$ was not observed. As was shown in earlier investigations¹⁰ of 5-MeV/u C^{6+} , O^{8+} , and $Ne^{10+} + He$ the singly differential cross sections agree with the PWBA predictions to within 40%. This points to a redistribution effect, or, in terms of quantum mechanics, the influence of polarization effects. Especially continuum-continuum couplings, i.e., transitions between different continuum states, seem to be of importance where electrons initially ejected into backward directions are attracted by the projectile and deflected into forward directions. This also explains the decreased cross section at backward angles compared to the PWBA. It should be noted that this effect hardly seems to be influenced by the electronic structure of the projectile (compare Figs. 2 and 4) or the target species (compare Figs. 2 and 3).

Figures 5(a)–5(c) display the energy dependence of the DDCS for 11 electron-observation angles in 6-MeV/u

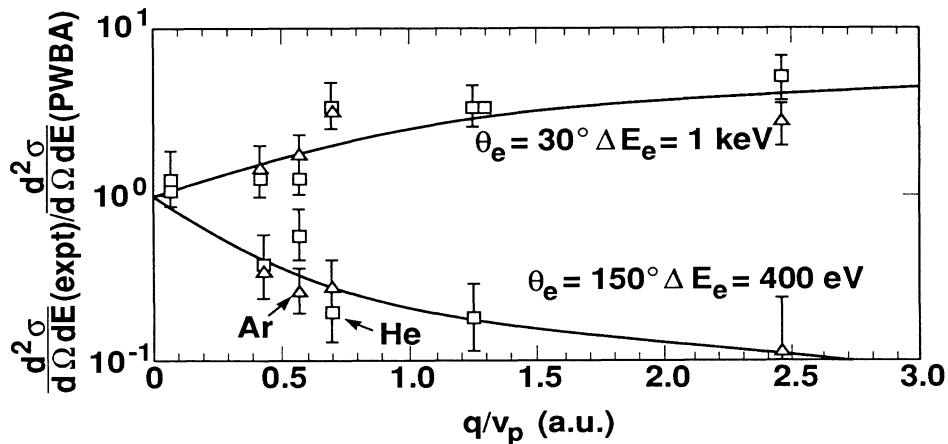


FIG. 6. Ratio of experimental to theoretical doubly-differential cross sections for two electron observation angles and energies as functions of q/v_p . The solid line is drawn to guide the eye.

$U^{38+} + Ar$ collisions. The experimental data are compared to theoretical results from two different CTMC codes. There is excellent agreement between the CTMC results and experimental data for ejection angles $< 110^\circ$. For an electron-ejection angle of 140° there seems to be a better agreement between experimental data and SCTMC results than between experimental data and n CTMC results. This might be an indication of the importance of the momentum distribution used to describe the initial state or the difficulty in accurately estimating the transition probabilities for small impact parameter collisions. In the n CTMC, a hydrogenlike distribution is used, whereas the SCTMC calculation starts with a distribution similar to a Hartree-Fock momentum distribution. However, both models are able to describe the ionization process rather accurately. This is because all interactions between projectile, target, and ejected electron are fully taken into account. This also includes polarization effects such as continuum-continuum couplings inferred from the comparison with sophisticated PWBA calculations.

Figure 6 shows the ratio of experimental DDCS to DDCS obtained from PWBA calculations for different collision systems. The ratio is scaled in accordance with the PWBA as a function of q/v_p projectile charge and velocity. For the present investigation q/v_p is 2.45. Data from previously published experiments^{4,5,10,11} (H^+ , C^{6+} , O^{8+} , Ne^{10+} , and Mo^{40+} on He and Ar) are also included. We have chosen one forward angle (30° at an electron energy of 1 keV) and an extreme backward angle (150° at an electron energy of 400 eV) for this comparison. The ratio clearly exhibits a q/v_p scaling. Since there is no significant difference between the ratios obtained for He and Ar targets, we conclude that the forward enhancement as well as the backward decrease might be target-

independent quantities. In fact, this might be expected if continuum-continuum couplings lead to a redistribution of the primary electron spectra (as given by PWBA calculations) for these fast-ion-atom collisions. Furthermore, Fig. 6 seems to display a saturation effect for high values of q/v_p . The reason for such a behavior could be another polarization effect such as, e.g., an increased binding.⁹

V. CONCLUSION

In conclusion, good agreement between experimental and theoretical doubly differential cross sections (n CTMC and SCTMC) is found for 6-MeV/u U^{38+} and Th^{38+} on He and Ar. It is evident from the comparison with PWBA predictions that polarization effects, especially continuum-continuum couplings, are important in these fast collisions for highly charged ions. Furthermore, there is evidence for a (target-independent) q/v_p scaling of the asymmetry with regard to backward and forward emission angles. This finding should be further investigated experimentally and has, as well, implications for further theoretical developments.

ACKNOWLEDGMENTS

The authors wish to express their gratitude for the efficient support through the basic atomic-physics research program at Lawrence Livermore National Laboratory and in particular to Dr. R. Fortner, Dr. R. Bauer, and Dr. H. Graboske. The support given to us by the Lawrence Berkeley Laboratory Super HILAC operator crew is greatly acknowledged. This work was performed under the auspices of the U.S. Department of Energy by the Lawrence Livermore National Laboratory under Contract No. W-7405-ENG-48.

*On leave from Hahn-Meitner-Institut, 1000 Berlin 39, West Germany.

¹M. E. Rudd and T. Jorgensen, Jr., *Phys. Rev.* **131**, 666 (1963); C. E. Kuyatt and T. Jorgensen, *ibid.* **130**, 140 (1963); M. E. Rudd, C. A. Sauter, and C. L. Bailey, *ibid.* **151**, 20 (1966).

²L. H. Toburen, *Phys. Rev. A* **3**, 216 (1971); L. H. Toburen and W. E. Wilson, *ibid.* **5**, 247 (1972).

³N. Stolterfoht, *Z. Phys.* **248**, 81 (1971).

⁴S. T. Manson, L. H. Toburen, D. H. Madison, and N. Stolterfoht, *Phys. Rev. A* **12**, 60 (1975); S. T. Manson (private communication).

⁵M. E. Rudd, L. H. Toburen, and N. Stolterfoht, *At. Data Nucl. Data Tables* **18**, 413 (1976).

⁶D. R. Gibson and I. D. Reid, *J. Phys. B* **19**, 3265 (1986).

⁷Y. K. Kim and M. Inokuti, *Phys. Rev. A* **12**, 1257 (1973).

⁸N. Stolterfoht, D. Schneider, D. Burch, H. Wiemann, and J. S. Risley, *Phys. Rev. Lett.* **33**, 59 (1974).

⁹G. Schiwietz, *Phys. Rev. A* **37**, 370 (1988).

¹⁰H. Platten, Ph.D. thesis, Hahn-Meitner-Institut, Berlin, West Germany, 1986 (unpublished); G. Schiwietz, H. Platten, D. Schneider, T. Schneider, W. Zeitz, K. Musiol, R. Kowallik, and N. Stolterfoht, Hahn-Meitner-Institut Report No. HMI-B447, Berlin (West), 1987 (unpublished); G. Schiwietz, B. Skogvall, N. Stolterfoht, D. Schneider, V. Montemayor and H. Platten, *Nucl. Instrum. Methods* (to be published).

¹¹D. Stolterfoht, D. Schneider, J. Tanis, H. Altevogt, A. Salin, P. D. Fainstein, R. Rivarola, J. P. Grandin, J. N. Scheurer, S.

Andriamonje, D. Bertault, and J. F. Chemin, *Euro. Phys. Lett.* **4**, 899 (1987).

¹²H. Schmidt-Böcking (private communication); R. E. Olson, *J. Phys. B* **12**, 1843 (1979).

¹³P. D. Fainstein and R. D. Rivarola, *J. Phys. B* **20**, 1285 (1987); R. D. Rivarola and P. D. Fainstein, *Nucl. Instrum. Methods* **B24/25**, 240 (1987).

¹⁴R. E. Olson, in *Electronic and Atomic Collisions*, edited by Gilbody *et al.* (North-Holland, Amsterdam, 1987).

¹⁵R. E. Olson, T. J. Gay, H. G. Berry, E. B. Hale, and V. D. Irby, *Phys. Rev. Lett.* **59**, 36 (1987).

¹⁶R. E. Olson and T. J. Gay, *Phys. Rev. Lett.* **61**, 302 (1988).

¹⁷J. Macek, *Phys. Rev. A* **1**, 235 (1970).

¹⁸G. B. Crooks and M. E. Rudd, *Phys. Rev. Lett.* **25**, 1599 (1970).

¹⁹A. Salin, *J. Phys. B* **2**, 631 (1969); **5**, 979 (1972); Dz. Belkic, R. Gayet, and A. Salin, *Phys. Rep.* **56**, 279 (1979).

²⁰G. Schiwietz and W. Fritsch, *J. Phys. B* **20**, 5463 (1987), and references therein.

²¹G. Schiwietz and V. Montemayor (unpublished).

²²R. E. Olson and A. Salop, *Phys. Rev. A* **16**, 531 (1977).

²³G. Schiwietz (unpublished). The calculations were performed according to Ref. 24 utilizing a generalized screened projectile potential.

²⁴D. R. Bates and G. Griffing, *Proc. Phys. Soc., London, Sect. A* **66**, 961 (1953).

²⁵C. O. Reinhold and R. E. Olson, *Phys. Rev. A* **39**, 3861 (1989).